

Adaptive Battery Diagnosis/Prognosis for Efficient Operation

Eugene Kim, Bin Wu, Kang Shin
University of Michigan
Ann Arbor, Michigan
{kimsun,wubin,kgshin}@umich.edu

Jinkyu Lee
Sungkyunkwan University
Suwon, Korea
jinkyu.lee@skku.edu

Liang He
University of Colorado
Denver, Colorado
liang.he@ucdenver.edu

ABSTRACT

Since most modern mobile and electric vehicles are powered by Lithium-ion batteries, they need advanced power management that jointly considers battery performance and related electrochemical reactions. To meet these needs, we develop a charging diagnosis and prognosis system for effective battery control. We first examine the battery model that can capture electrochemical reactions and battery performance. Based on this model, we develop a charging diagnosis system that determines battery internal states and predicts their trend over operational cycles in various environments. Next, we propose a prognosis system to estimate battery's *end-of-life* (EOL) and determine optimal operating environments. Our in-depth experiments demonstrate that the proposed diagnosis and prognosis system estimates battery parameters and their degradation over operational cycles in various environments with high accuracy and without degrading user-perceived experience.

CCS CONCEPTS

• **Hardware** → **Batteries**.

ACM Reference Format:

Eugene Kim, Bin Wu, Kang Shin, Jinkyu Lee, and Liang He. 2019. Adaptive Battery Diagnosis/Prognosis for Efficient Operation. In *Proceedings of the Tenth ACM International Conference on Future Energy Systems (e-Energy '19)*, June 25–28, 2019, Phoenix, AZ, USA. ACM, New York, NY, USA, 10 pages. <https://doi.org/10.1145/3307772.3328286>

1 INTRODUCTION

Lithium-ion batteries have been widely used in mobile devices, drones, and electric vehicles (EVs), thanks mainly to their high energy-density and long service-life [1]. Battery diagnosis and prognosis — via accurate estimation of battery characteristics, such as maximum power capability and end-of-life (EOL) [1–4] — are crucial to their reliable operation [5, 6]. Therefore, a standard procedure for battery management system (BMS) designers, especially in automotive industry, is to (i) test and evaluate battery performance in terms of energy capacity and internal resistance in different operating environments, and tabulate the battery performance parameters along with the associated operating conditions; (ii) based on these parameters, determine efficient and safe operating conditions within which the batteries can power the system without

suffering fast capacity degradation or quick increase of internal resistance; and (iii) estimate battery states and operating conditions to keep the batteries efficient and safe after the (mobile or vehicle) product is released.

However, offline battery characterization and model parameters' calibration cannot accurately capture the battery degradation pattern under various operating conditions. Vehicles operate under different temperature (T), voltage (V) discharge/charge-rate (I), etc., and at different regions/countries or by different drivers throughout their warranty periods. Also, every battery has its own dynamics and degradation characteristics [7]. So, the battery degradation pattern identified offline is unlikely to hold for all batteries throughout their warranty periods, thus necessitating the online construction of a battery degradation model that captures the effect of operating conditions [6].

The challenges in building such an online battery degradation model are three-fold. First, it requires a comprehensive understanding of battery operation, which is a rather complex electro-chemical process that affects the battery's energy efficiency in many aspects. Second, most efficiency-related battery parameters change over time, and thus the parameters dominating battery degradation, together with their relationship with batteries' operating conditions (i.e., V, I, T), must be identified and used in real time. This is because the operating conditions affect batteries' internal electrochemical reactions — and thus their efficiency and degradation — significantly, rendering battery degradation a complex process. This renders simple battery models unable to describe/predict their current/future state-of-health (SOH) [3, 6]. Third, direct checking of the material state of a battery is expensive and destructive, e.g., disassembling a battery pack entails additional labor and cost. An ideal battery diagnosis/prognosis system must be able to estimate battery SOH in a pack without taking intrusive measures nor requiring a significant amount of time, both of which degrade user-perceived experience.

There have been numerous ways to estimate battery SOH by identifying battery degradation states with non-destructive data-driven approaches [1, 4, 8–11]. Most of them assessed battery SOH in terms of energy capacity and direct current internal resistance (DCIR). Based on the degradation profiles of battery's energy capacity and internal resistance under different operating conditions, they construct a degradation model as a function of operating conditions and cycles/time using pre-defined mathematical functions such as exponential and/or polynomial functions. Battery's energy capacity and internal resistance, albeit crucial, cannot fully represent the important parameters that affect battery SOH. The authors of [3] proposed a comprehensive degradation model based on a physical electro-chemical model and validated it in several domains. However, applying their model in the real world requires certain cell information related to the electro-chemical battery model, which

Permission to make digital or hard copies of all or part of this work for personal or classroom use is granted without fee provided that copies are not made or distributed for profit or commercial advantage and that copies bear this notice and the full citation on the first page. Copyrights for components of this work owned by others than ACM must be honored. Abstracting with credit is permitted. To copy otherwise, or republish, to post on servers or to redistribute to lists, requires prior specific permission and/or a fee. Request permissions from permissions@acm.org.

e-Energy '19, June 25–28, 2019, Phoenix, AZ, USA

© 2019 Association for Computing Machinery.

ACM ISBN 978-1-4503-6671-7/19/06...\$15.00

<https://doi.org/10.1145/3307772.3328286>

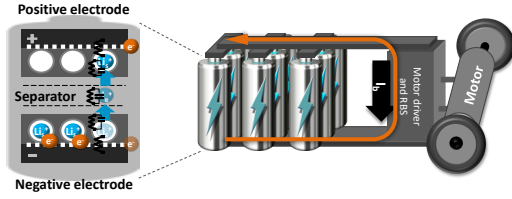


Figure 1: Discharging process of Li-ion batteries.

is usually proprietary to battery cell manufacturers and thus has limited availability.

In this paper, we propose an adaptive battery diagnosis/prognosis system for efficient battery control via charging diagnosis and using a newly-constructed adaptive battery degradation model. This system monitors battery behavior while charging, which is then used to estimate battery SOH parameters. The thus-obtained SOH parameter profiles are recorded along with the corresponding number of operation cycles and the operating conditions (V, I, T), which will be logged on the server. Based on the logged data, we explore a degradation model-form and derive model parameters which capture the relationship between the performance degradation rates and the operating conditions applicable to any type of battery used in vehicles/mobile systems. The resulting degradation model allows the BMS to predict battery EOL (end-of-life) and search for the optimal battery operating conditions so as to maximize battery performance within a given warranty period.

This paper makes the following main contributions:

- proposal of a diagnostic charging system that identifies and collects battery SOH information during charging based on half-cell open-circuit voltage curves without any other prior electrochemical knowledge;
- development of a free-form battery degradation model based on the logged data via generic model-form search;
- creation of an adaptive parameter model in the degradation model over a wide range of operation conditions through a support vector regression;
- prediction of battery EOL based on the constructed degradation model; and
- construction of a holistic framework for battery diagnosis/prognosis and demonstration of its efficiency via in-depth experimentation.

The rest of this paper is organized as follows. Sec. 2 provides the background of battery model and degradation, and Sec. 3 formally states our problem and solution approach. Sec. 4 describes how to estimate the battery model parameters related to battery performance and SOH during charging. Sec. 5 describes the construction of battery degradation models for predicting batteries' future states and their use to predict battery EOL. Sec. 6 evaluates the proposed battery diagnosis/prognosis system. The paper concludes in Sec. 7.

2 BACKGROUND

We present the necessary background of battery management.

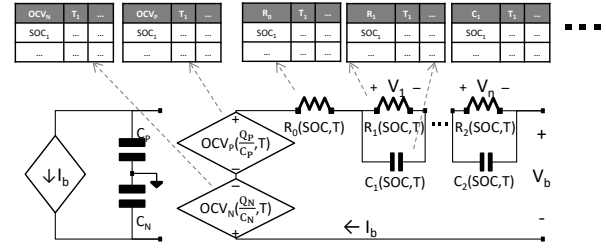


Figure 2: Equivalent circuit battery model.

2.1 Li-ion Battery Operation and Modeling

Let us first consider how battery operates during discharging and charging. When discharging a battery, Li-ions in the active materials of its negative electrode (i) diffuse to the surface and move from the solid phase to the electrolyte phase; and then (ii) travel through electrolyte and enter inside the active material in the positive electrode. During this process, the electrons released in the negative electrode travel through the external circuit to generate a flow of current, as shown in Fig. 1. This process occurring in the positive and negative electrodes will be reversed during charging. When current flows through a battery cell during discharging/charging, there are a number of factors causing its voltage drops from the equilibrium open-circuit voltage (OCV) — commonly called “overpotential”, including: (i) ohmic drop due to electronic or ionic current flow (i.e., Ohm’s law), (ii) concentration overpotential due to the buildup of concentration gradients in a battery, and (iii) surface overpotential needed to drive the reactions. Based on the overpotential and operating principles of battery, we develop the equivalent circuit model consisting of a parametric open circuit voltage model and electronic components shown in Fig. 2.

2.1.1 Equivalent Circuit Model. Typically, a large capacitor or a dependent voltage source is used to represent OCV. We use two different capacitors and dependent voltage sources to analyze OCV based on positive and negative electrodes characteristics. These characteristics include energy capacities and OCV–SOC relations, which are detailed in the next section. The rest of the circuit simulates (i) the battery’s ohmic resistance (R_0) due to the ohmic and surface overpotential, and (ii) the dynamic voltage behaviors ($R_1, C_1, \dots, R_n, C_n$) caused by the concentration overpotential when battery is discharged/charged at the rate I_b . These battery parameters (i.e., OCV, R_0, R_1, C_1, \dots) are representative of a particular battery type, and is, in general, a nonlinear function of state-of-charge (SOC) and temperature (T) [4]. The number of RC branches in the equivalent circuit model determines the model’s accuracy and complexity. In this paper, we use the most dominant RC branch (R_1, C_1) to describe the dynamic voltage behavior for simplicity.

2.1.2 Parametric Open-Circuit Voltage (OCV) Model. Battery capacity is dictated by the capacities of positive and negative electrodes (C_P, C_N), and these capacities can be estimated using OCV measurement and OCV characteristics of positive and negative electrodes (OCV_P, OCV_N). The parametric OCV model has been proposed to analyze the battery’s entire OCV based on the stored charge capacity (Q_N, Q_P) and the total maximum charge capacity (C_N, C_P) [12, 13] as:

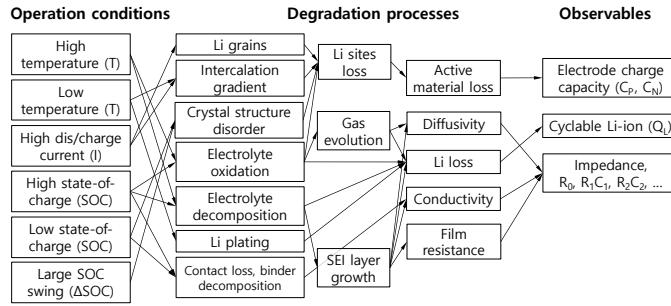


Figure 3: Degradation factors and their impacts [3, 14]

$$\begin{aligned} \text{OCV} &= \text{OCV}_P \left(\frac{Q_L^P}{C_P} \right) + \text{OCV}_N \left(\frac{Q_L^N}{C_N} \right) \\ Q_L &= Q_L^P + Q_L^N, \end{aligned} \quad (1)$$

where Q_L^P and Q_L^N are the amounts of Li-ion that are inter-calated in positive and negative electrodes' active material, respectively, and C_P and C_N are the maximum charge capacities of the active materials to store Li-ions without over/under-voltage in the positive and negative electrodes, respectively. Based on the parametric OCV model, the battery's total charge capacity can be assessed with 3 important parameters: the capacity of positive and negative active material (C_P and C_N), and the amount of cyclable Li-ion (Q_L). These parameters decrease slowly over time due to side chemical reactions in the battery.

2.2 Changes of Battery Parameters due to Degradation

Battery performance degrades over cycles/time, observed as not only charge capacity decrease, but also as internal resistance increase (R_0, R_1) and capacitance decrease (C_1). Increased internal resistance leads to larger voltage drop, and decreased internal capacitance makes such drop faster, both degrading battery's power capability. Note that we extract the most dominant R_1 – C_1 pair with the largest resistance in the RC pairs for the model. The changes of these parameters rely heavily on battery's operating conditions as shown in Fig. 3, including high/low temperature, high/low SOC, large charge/discharge current, frequent discharge/charge cycles, etc., which accelerate the side chemical reactions related to solid electrolyte interfaces (SEI) layer growth, lithium plating, gas and precipitation generation, electrolyte oxidation and decomposition [3, 14]. Along with these chemical side reactions, mechanical stress on the electrodes during charge/discharge cycles also leads to contact loss, particle cracking, and structure disorder. These chemical and mechanical stresses affect the parameters closely related to battery performance over cycles.

3 PROBLEM STATEMENT AND PROPOSED APPROACH

Thus far, we have discussed the necessary background of the battery model, state-of-health (SOH) and degradation factors. Electrodes'

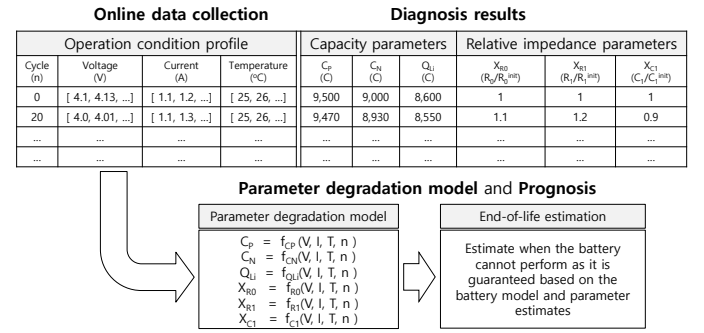


Figure 4: Overall process for the proposed diagnosis/prognosis. Capacity unit, Coulomb (C), is defined as the quantity of electric charge carried in 1 second (s) by a current of 1 ampere (A)

capacities (C_P, C_N) and the amount of Li-ion (Q_L) must be identified as they are closely related to the battery's energy capacity. We must also extract the battery's internal resistances (R_0, R_1) and capacitance (C_1) to describe its dynamic behavior such as voltage drop and recovery effect. Moreover, the degradation of these parameters over time is affected by the battery's operating condition (V, I, T). Therefore, the underlying diagnosis system must identify them accurately, and the prognosis system should capture the relationship between their degradation and the operating condition (V, I, T). Presented below are a formal statement of our diagnosis/prognosis problem and the overview of our proposed solution.

3.1 Problem Statement

With the above system model, assumptions and notations, our problem can be formally stated as:

Using battery data measured in the charging titration period, Develop a battery diagnosis/prognosis system that identifies the battery parameters related to the energy capacities (C_P, C_N, Q_L) and internal resistances (R_0, R_1, C_1), determine the battery parameters' degradation rates and establish the relationship between and the operating condition (V, I, T) and the parameters' degradation rates so as to predict *battery degradation pattern* and *end-of-life (EOL)*, and optimize *battery operating condition* (V, I, T).

Considering users' convenience and cost, the diagnosis system should be able to estimate parameters ($C_P, C_N, Q_L, R_0, R_1, C_1$) based only on measured data without disassembling a battery pack or any other destructive measurements. The prognosis system must complete the development of a battery degradation model based on the diagnostic data.

3.2 Overview of Proposed Solution

Fig. 4 shows the overall diagnosis/prognosis process. First, battery current–voltage characteristics are captured periodically through a titration technique [15]. Based on these characteristics, the model parameters are estimated and stored in tables with the corresponding operating conditions (V, I, T) and the number of cycles (n). For this step, the system needs a parameter estimation technique,

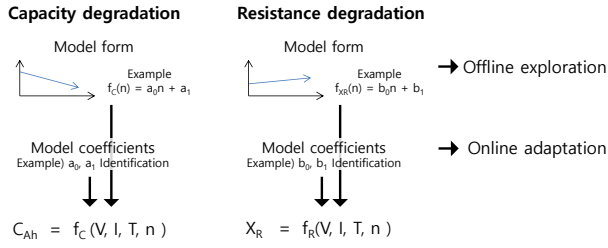


Figure 5: Conventional modeling of battery degradation.

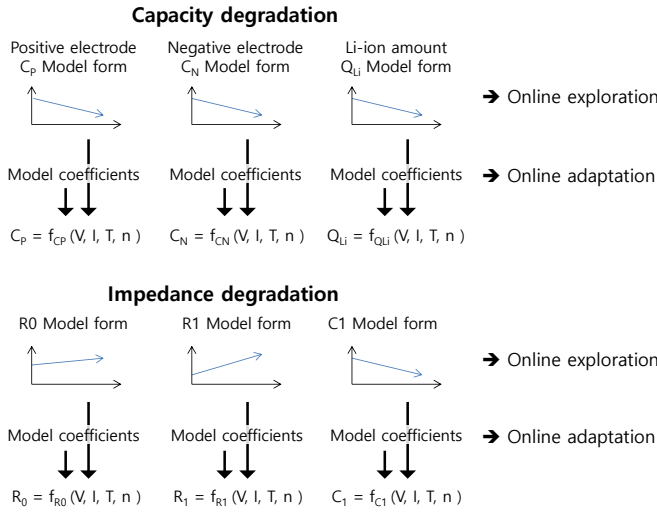


Figure 6: Proposed modeling of battery degradation.

which will be detailed later. The prognosis system then develops the battery degradation model based on the collected diagnosis information. The degradation model, in turn, is used to predict battery's *end-of-life* (EOL), defined as when the battery performance has dropped significant enough (e.g., to 50~80% of its initial capacity [16, 17]). Here, we use 70% of the initial energy capacity as EOL. Also, the degradation model with respect to operating conditions allows the BMS to search for “effective” operating conditions to ensure smooth system operation throughout the warranty period.

3.3 State-of-the-Arts and Their Limitations

Various approaches to parameter identification have been developed over the last decade or so. Electrical parameter estimation via electrochemical impedance spectroscopy (EIS) and time constant analysis are well-known to describe the dynamic voltage transient with respect to discharge/charge current [18–20]. A parametric OCV model was proposed to determine the battery's active material capacities and the amount of cyclable Li-ion [12, 13]. We propose the battery diagnosis system that facilitates parameter estimation for battery management and prognosis, especially for EVs. We first introduce the applicable battery diagnosis techniques, and then develop applicable algorithms for real vehicles. For battery prognosis, most existing studies of battery degradation search for

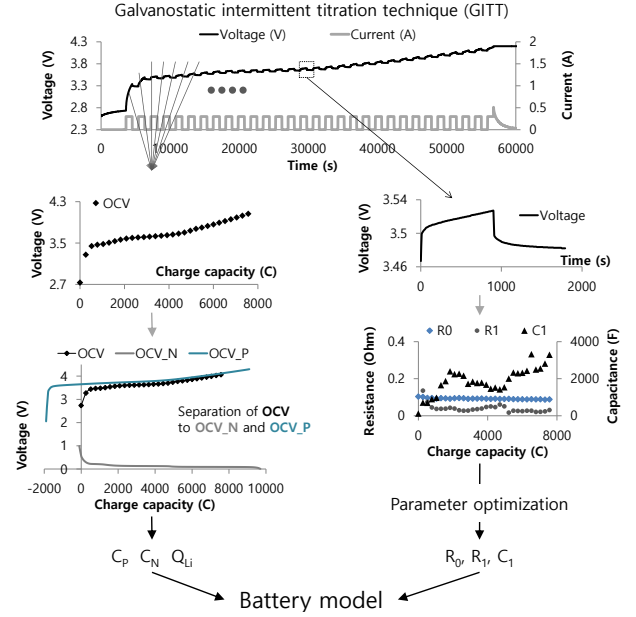


Figure 7: Model-based battery diagnosis

the optimal model coefficients of the pre-defined form of degradation model as shown in Fig. 5 [1, 4, 8, 10, 11]. The pre-defined models are selected based on the observations from a large number of offline degradation tests under various operating conditions. To describe the non-linear property of battery degradation, they used exponential, polynomial, or power functions, because these functions can fit the degradation patterns in their test environments. A non-linear regression or neural network was utilized to identify the coefficients of the pre-defined model.

Fig. 6 shows the overall procedure of our modeling of battery degradation. Instead of battery's total capacity and internal resistance, we develop a more detailed degradation model consisting of positive/negative electrode capacity, resistances and capacitance. Also, to construct a more adaptive degradation model, we take an additional step to select a generic model-form instead of using a pre-defined model form. In addition to identifying degradation patterns, the system also focuses on the impact of operating conditions on the battery degradation rate as:

$$D_x = f_x(V, I, T),$$

where x is the battery model parameters including $\{C_p, C_n, Q_L, R_0, R_1, C_1\}$ and D_x is the degradation rate of x . $\{V, I, T\}$ are measurable and controllable operating conditions related to battery degradation.

4 DIAGNOSTIC CHARGING SYSTEM

We now detail the battery diagnostic charging system in which the amount and duration of charge current are controllable. Fig. 7 shows an example diagnosis procedure to estimate the battery model parameters.

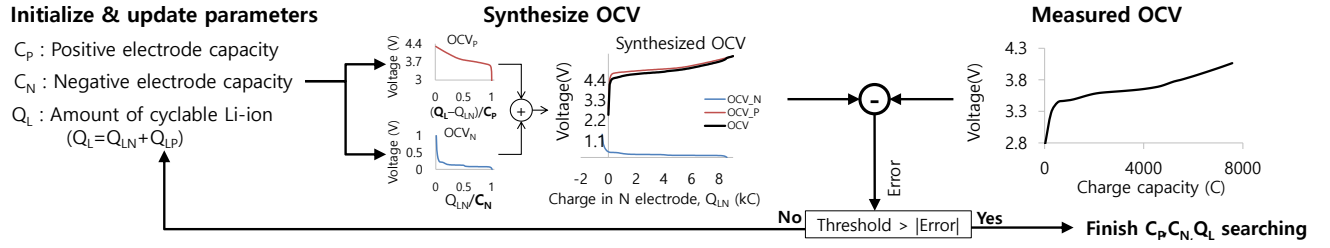


Figure 8: Model-based battery OCV parameter estimation.

4.1 Parameter Estimation of Equivalent Circuit Battery Model

The titration procedure in the algorithm normally consists of a series of charge current pulses, followed by a relaxation time. During a charge current pulse, the battery voltage first quickly increases by a value proportional to its ohmic internal resistance (R_0), and then the voltage slowly increases further due to the constant charge pulse and a charge migration and diffusion effect which is described by additional resistance and capacitance (R_1, C_1, \dots). We record these voltage changes to estimate battery internal parameters (R_0, R_1, C_1). Based on the captured voltage–current characteristics, we determine $R_0(\text{SOC}, T)$, $R_1(\text{SOC}, T)$, $C_1(\text{SOC}, T)$ over battery SOC and temperature T [4] as shown in Fig. 7. After a charging period, during the relaxation time, the voltage first suddenly decreases to a value proportional to the internal resistance (R_0), and then slowly decreases until output voltage in equilibrium is reached. These equilibrated voltages are recorded since they are close to the battery's open circuit voltage (OCV(SOC, T)) at the corresponding SOC and temperature (T) levels. This charge-and-relaxation procedure is applied repeatedly until the battery is fully charged ($V_o = 4.2\text{V}$), acquiring the OCV characteristics over a full range of battery SOC.

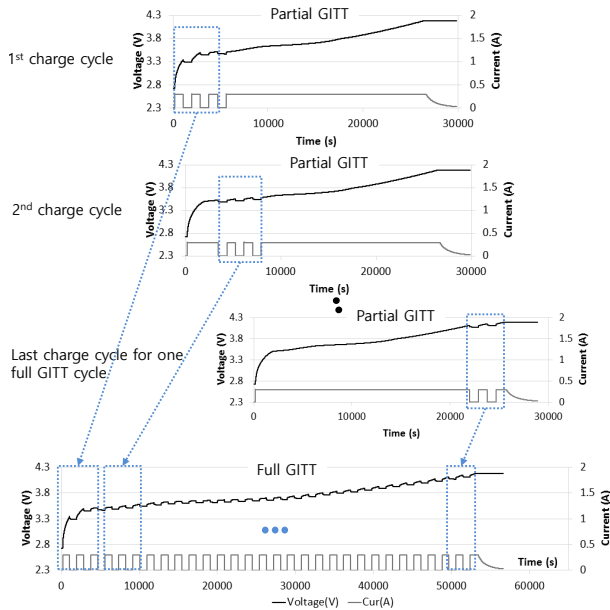


Figure 9: GITT for the system over the full range of SOC.

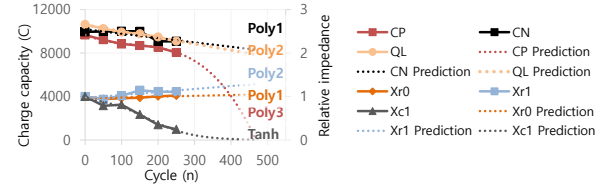


Figure 10: Example model parameter degradations during 250 discharge/charge cycles. Operating temperature is 23°C , battery C-rate is 2,300mA, charge current is 2A, max voltage is 4.2V, average discharge current ($E(I_d)$) is 2A, and the root mean square of discharge current ($RMS(I_d)$) is 2.45A. Dotted lines show the degradation predictions of model parameters. These graphs are obtained with evaluation process to be described in Section VI.

4.2 Estimation of OCV Model Parameters

Battery electrodes' capacities and cyclable Li-ion amount decrease over time due to side chemical reactions in the battery. While the battery's maximum capacity decreases, the SOC and OCV will change faster even with the same charge current. The parametric OCV model enables the analysis of battery OCV in terms of active materials' charge capacities based on these relations between OCVs (OCV_P, OCV_N) and SOC ($\frac{Q_P}{C_P}, \frac{Q_N}{C_N}$). Fig. 8 presents a search procedure for C_P, C_N, Q_L based on the OCV–charge capacity curves ($OCV_P(x)$ and $OCV_N(x)$) [12, 13].

We synthesize the OCV curve based on OCV_P and OCV_N with the capacity parameters (C_P, C_N, Q_L). Battery $OCV_N(\frac{Q_L^N}{C_N})$ and $OCV_P(\frac{Q_L^P}{C_P})$ depend on active materials' maximum charge capacity (C_P, C_N) and the amount of charge (Q_L^N, Q_L^P) in the active materials [12, 13]. Note that the $OCV_N(\frac{Q_L^N}{C_N})$ and $OCV_P(\frac{Q_L^P}{C_P})$ curves are very different functions in terms of charge concentration ($\frac{Q_L}{C}$) [12, 13]. Next, we compare the measured and synthesized OCVs with respect to the charge capacity (Q). The algorithm continues searching the parameter set (C_P, C_N, Q_L) until the difference between the measured and synthesized OCVs becomes smaller than the pre-specified value.

4.3 Diagnostic Charging System

One may wonder if a series of charge current pulses may prolong the time to fully charge the vehicle's batteries and thus degrade users' experience. We address this concern by only applying the

charge current pulses during night when EV batteries are charged from the wall power while being parked. Also, a few hours may not be sufficient to apply the entire series of charge current pulses; we divide the series into several intervals, which can be applied on different days. This is valid because battery behaviors are similar over several consecutive days as shown in Fig. 9.

For the first charge cycle, partial GITT (Galvanostatic intermittent titration technique, as shown in Fig. 7) is performed for diagnosis at the lowest SOC. In case the system cannot perform GITT over the full SoC range due to limited charge time, GITT is applied only to a partial SoC range. While following charge cycles, the charge system applies GITT to identify battery parameters at other SoC ranges until the system collects the full SOC range of diagnostic information. Fig. 10 shows an example of parameter estimation during the first 250 cycles.

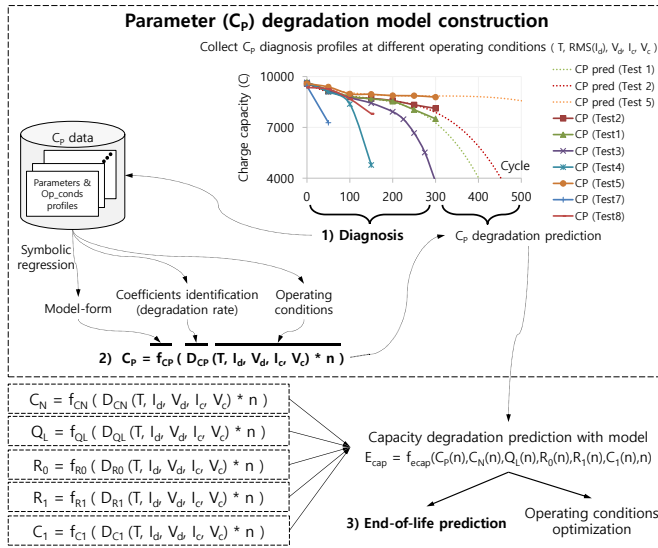


Figure 11: Overall procedure of battery prognosis: 1) Performance parameter estimation via periodic charging diagnosis and parameters storage into a server; 2) Parameter degradation modeling based on the stored performance parameters; 3) End-of-life (EOL) prediction based on the parameter degradation and battery models introduced in 2

5 PROGNOSIS SYSTEM

Thus far, we have explored the diagnosis of battery model parameters related to SOH and performance. Next we propose how to prognose the battery based on the diagnosis results, and handle the case when the battery is expected to die before the warranty expires. Fig. 11 shows the overall procedure for the proposed battery prognosis system. First, the system constructs the battery degradation models adaptively to operating conditions. Then, the system predicts the battery EOL and regulates the operating conditions so as to maximize battery performance within the warranty period.

5.1 Adaptive Performance Degradation Model

The degradation state (S) includes the charge capacity parameters (C_P, C_N, Q_L), and relative internal resistances and capacitances ($X_{R_0}, X_{R_1}, X_{C_1}, \dots$). The parameter degradation models (f_S) can be represented by functions of operating conditions and the number of cycles (n) as:

$$\begin{aligned} S &= (C_P, C_N, Q_L, X_{R_0}, X_{R_1}, X_{C_1}, \dots), \\ &= f_S(D_S(\mathbf{x}) \cdot n), \\ \mathbf{x} &= [T, RMS(I_d), V_d, V_c, I_c], \end{aligned}$$

where \mathbf{x} is an operating condition vector including battery temperature (T), discharge stress ($RMS(I_d)$), minimum discharge voltage (V_d), maximum charge voltage (V_c) and charge current (I_c). Fig. 11 shows an overview of our approach to building the parameter degradation models. The proposed diagnosis system extracts and stores battery parameters with the corresponding operating conditions, and then uses the stored data to construct the battery degradation model by (i) applying a symbolic regression to construct the generic model form of parameter degradation profiles, and then (ii) constructing the degradation model (f_S) via fitting the coefficients (D_S) of the generic model. Note that the coefficients (D_S) need to be regressed with the operating conditions (\mathbf{x}) to account for their impacts on the parameter degradation rates. The thus-constructed model also facilitates prediction of battery EOL, which will be detailed later.

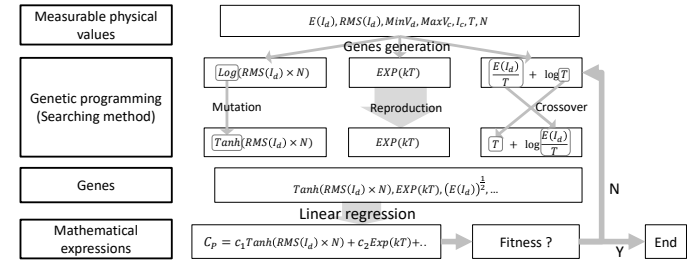


Figure 12: An example parameter function regression.

5.1.1 Generic Model-Form of Parameter Degradation. Fig. 10 shows battery parameters with degradation patterns. We first mathematically describe the degradation of battery parameters. Note that some mathematical functions are commonly used in electrochemical behavior modeling. For example, exponential and logarithmic functions are utilized in modeling various chemical reaction processes [5, 10, 11, 21]. Polynomial, hyperbolic functions are also exploited to describe the trend of physical quantities related to electrochemical reactions. Battery performance degradation is due mainly to chemical reactions, and hence a combination of these functions must be used to describe the degradation patterns.

The symbolic regression with polynomial, exponential, logarithmic and hyperbolic functions is performed to find a generic model-form of degradation based on many degradation profiles of batteries stored in a server. We initially selected a linear parameter model which is then evaluated in terms of its fitness with the collected data. If the fitness is not met, other models are explored in the search space. A more effective model is searched for

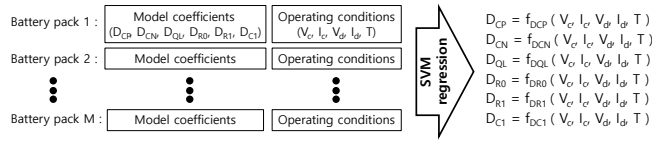


Figure 13: Development of the parameter degradation rate function based on parameter degradation and operating condition profiles.

via genetic programming, which is based on an evolutionary algorithm [22, 23]. In genetic programming, candidate models are created for the next generation via a mutation and a crossover based on the parents' models with low weights. We reproduced models with large weights to leave the genes that are likely to critically affect the model. The system evaluates its fitness and repeatedly generates new generations until the fitness is satisfied.

5.1.2 Regression of Parameter Degradation Rate. Battery degradation depends on the operating condition, such as temperature, dis/charge current and operating voltage range. To customize the parameter degradation model-form while considering the operating conditions, BMS must regress the parameters related to degradation rate over the operating conditions. Based on such a degradation rate under the corresponding operating conditions, we can find a degradation model function that represents the impact of the operating conditions on parameter degradation. To regress the parameters of the degradation rate model, neural network regression and support vector regression with Gaussian, polynomial and linear functions can be used on the recored battery degradation data as seen in Fig 13.

5.2 Battery Capacity Degradation and EOL Prediction

Described below is how battery performance degradation can be estimated based on the parameter degradation trends and operating conditions. Then, we can identify when the battery capacity drop below the EOL capacity (70% of their initial capacity) as shown in Fig. 15.

5.2.1 Performance Estimation Based on Parameter Degradation Estimation. Based on the parameter degradation models, the performance degradation over cycles can be estimated. Energy capacity is the most important metric, and is defined as the available amount of energy while maintaining voltage within an acceptable range. Hence, the energy capacity can be assessed based on the OCV curve and the current level for the underlying application. Fig. 14 shows an example of energy capacity estimation. A decreased energy capacity causes battery to reach the voltage limit more quickly even with the same current. The internal resistance also accelerates the decrease of energy capacity because a larger resistance may incur a larger voltage drop, thereby causing an earlier voltage drop (or rise) below the minimum (or above the maximum) required value. The energy capacity can be assessed based on the total charged capacity by integrating the current over time in the test profiles.

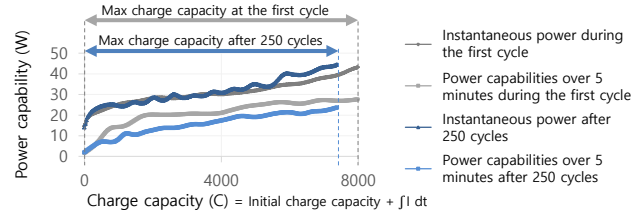


Figure 14: Example total capacity and power capability degradations. After 250 cycles, the battery's energy capacity and power capability over 5 minutes decrease.

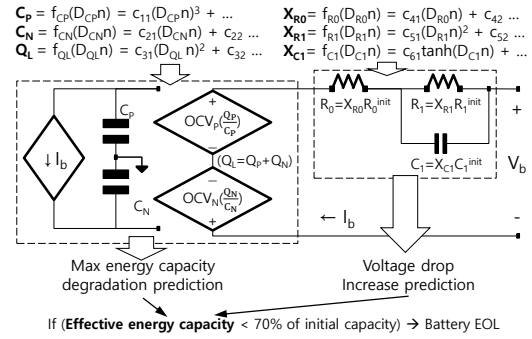


Figure 15: Battery EOL prediction based on the battery model and the model parameter degradation function

5.2.2 EOL Prediction. Fig. 15 shows the algorithm for prediction of battery EOL. First, the degradation of model parameters over cycles can be predicted by using the degradation model. Then, we can estimate energy capacity degradation and internal resistance increase based on the battery model and parameter degradation estimations. Note that, in most applications, battery EOL is defined as the point at which the a battery will hold only a pre-set percentage (70%) of its original storage capacity. Therefore, we can search for battery EOL by identifying the number of cycles where the energy capacity is estimated to drop below the 70% of its initial capacity.

5.2.3 Determination of Operating Condition Bounds. The parameter degradation models tell not only the total capacity degradation under current operating conditions, but also the relationship between operating conditions and the parameter degradation rate. Therefore, the model can be used to optimize the operating condition bounds to guarantee the battery warranty while providing the required power capability and energy capacity. For example, if the estimated battery EOL is shorter than the warranty period, the operating condition bounds must be regulated to decelerate battery degradation at the expense of the battery's effective capacity. *Effective charge capacity, Q_{eff}* , can be calculated by considering the total charge capacity (C_Q) and charge loss (Q_{loss}^{Id} , Q_{loss}^T) due to the regulation of operating conditions ($Q_{eff} = C_Q - Q_{loss}^{Id} - Q_{loss}^T$). To regulate $RMS(I_d)$, an energy buffer is required to move charges to the energy buffer temporarily through a DC/DC converter, leading to the loss of available charge as:

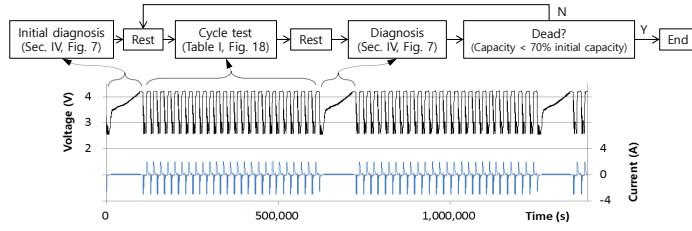


Figure 16: Test procedure for the diagnostic charging system introduced in Sec. 4 with different test cycle profiles. Tested cycle profiles are listed in Table 1

$$Q_{loss}^{I_d} = (1 - \eta_d)(1 - \eta_c)(RMS(I_d^{init}) - RMS(I_d)) t_{op},$$

where t_{op} is the operation time, η_d and η_c are charge-transfer efficiencies, $RMS(I_d^{init})$ and $RMS(I_d)$ are initial and target discharge stresses. Thermal control also consumes energy as:

$$Q_{loss}^T = \frac{1}{\eta_{th}}(T_{ext} - T) t_{op},$$

where η_{th} is a thermal efficiency, and T_{ext} is an external temperature. With the above system model, assumptions and notations, our problem can be stated formally as:

$$\begin{aligned} & \underset{\mathbf{x}}{\text{maximize}} && \alpha Q_{eff}(\mathbf{x}) + \beta S_{chg}(\mathbf{x}) \\ & \text{subject to} && EOL_{margin} + EOL_{req} < EOL_{model}(\mathbf{x}) \end{aligned}$$

where \mathbf{x} is $\{RMS(I_d), I_c, V_c, V_d, T\}$, S_{chg} is the charging time, EOL_{model} and EOL are estimated by the degradation model, EOL_{req} and EOL_{margin} are the required period of EOL and its margin. α and β are the weight of effective charge capacity and the required charge time, respectively. The charging speed can be assessed by total capacity (C_Q) and charge current (I_c) as:

$$S_{chg} = \frac{C_Q}{I_c}.$$

6 EVALUATION

We have evaluated the proposed battery model construction, EOL prediction, and operating conditions optimization via extensive experiments, lasting 8 months cumulatively.

6.1 Methodologies and Settings

Fig. 16 shows our testing procedure, which is implemented with the Neware's battery tester as shown in Fig. 17 and Li-ion batteries (18650, 2200 mAh) [24]. The battery discharge/charge current and output voltage are logged at 10 Hz during the tests, based on which the proposed model construction is evaluated. We intermittently diagnosed batteries to extract their characteristics, and saved the diagnostic results with the corresponding cycle and operating conditions. This procedure is repeated until the batteries reach their EOLs.

Due to the limited number of the battery tester's channels and the large number of required cycles to reach EOL, we collected battery degradation data under a selective range of operating conditions; temperature (T : 23–40 °C), discharge stress ($RMS(I_d)$: 2–4 A),



Figure 17: Neware battery tester

charge voltage (V_c : 4.1–4.3 V) and current (I_c : 1–4 A) are selected. We picked test voltage and current conditions based on charge capacity (C-rate) and recommended operating range. Additionally, our thermal chambers are used to account for temperature test conditions. These are summarized in Table 1 and Fig. 21. In future, we would like to investigate the impact of depth-of-discharge (affecting V_d) and a wider rate of testing conditions for temperature, RMS of discharge current, charge voltage and current.

Table 1: Profiles in battery testing.

| | T (°C) | V_d (V) | $RMS(I_d)$ (A) | V_c (V) | I_c (A) |
|----------------|----------|-----------|----------------|-----------|-----------|
| Test-1 | 23 | 2.6 | 2.00 | 4.2 | 2 |
| Test-2 | 23 | 2.6 | 2.45 | 4.2 | 2 |
| Test-3 | 23 | 2.6 | 3.65 | 4.2 | 2 |
| Test-4 | 23 | 2.6 | 2.45 | 4.3 | 2 |
| Test-5 | 23 | 2.6 | 2.45 | 4.1 | 2 |
| Test-6 | 40 | 2.6 | 2.45 | 4.2 | 2 |
| Test-7 | 23 | 2.6 | 2.45 | 4.2 | 4 |
| Test-8 | 23 | 2.6 | 4.00 | 4.2 | 2 |
| Test-9 | 23 | 2.6 | 3.65 | 4.2 | 2 |
| Test-10 | 40 | 2.6 | 2.45 | 4.2 | 2 |
| Test-11 | 23 | 2.6 | 2.45 | 4.2 | 3 |
| Test-12 | 23 | 2.6 | 2.45 | 4.1 | 2 |
| Test-13 | 40 | 2.6 | 3.65 | 4.2 | 2 |
| Test-14 | 23 | 2.6 | 2.45 | 4.3 | 1 |
| Test-15 | 40 | 2.6 | 2.45 | 4.2 | 1 |
| Test-16 | 23 | 2.6 | 2.85 | 4.2 | 2 |

6.2 Results

6.2.1 Degradation Patterns and Model. We evaluate the following three schemes for modeling battery degradation:

- EXP2-Const: the capacity degradation model based on two exponential functions [5, 21],
- EXP-PW: the capacity degradation model via exponential and power functions [10, 11], and
- SYMR: our capacity degradation model using the symbolic regression described in Section 5.1.

The batteries' measured initial capacities are about 8500 C (\approx 2300 mAh). So, their EOLs are reached when their capacities reduce to $8500 \times 70\% \approx 6000$ C (\approx 1667 mAh). Fig. 18 plots the prediction of capacity degradation starting at about 80% and 90% SOH with the above three schemes, respectively. The EOL is also predicted when the

battery is of 95%, 85%, and 75% remaining energy capacity, as summarized in Table 2. All three schemes predict EOL more accurately at later cycles, and SYMR achieves the best accuracy in all cases.

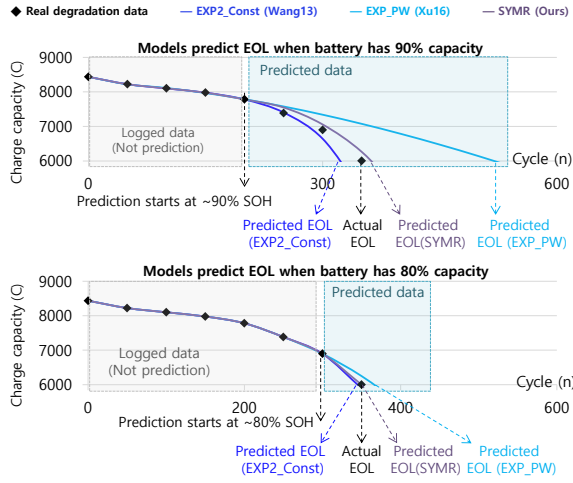


Figure 18: Examples of EOL prediction at different SOH

Table 2: Errors in predicting battery EOL

| EOL prediction start | EOL prediction error (%) | | |
|--------------------------|--------------------------|--------|------|
| Remaining capacity (SOH) | EXP2-Const | EXP-PW | SYMR |
| 95% | 43.8 | 251.2 | 26.1 |
| 90% | 40.6 | 73.9 | 16.5 |
| 85% | 19.9 | 17.5 | 5.5 |
| 80% | 9.4 | 10.4 | 5.4 |
| 75% | 10.8 | 8.4 | 2.2 |

6.2.2 Parameter Degradation Rate. Fig. 20 shows an example degradation parameter function (D_{CP}) with respect to the operating conditions. Fig. 20 (a) shows the impact of the charge current (I_c) and charge voltage (V_c) on degradation coefficients in the model while keeping other conditions intact, and Fig. 20 alc(b) shows the impact of temperature (T) and discharge/charge stress ($RMS(I_d)$) on the coefficient. Based on the degradation rate function, we can determine the impact of the operating conditions on the parameter degradation rate. This parameter degradation model is used to estimate EOL over a wide range of operation conditions as shown in Fig. 19 and schedule efficient operating conditions to improve system performance.

6.2.3 Determination of Operation Bounds. Using the battery parameter degradation model, we optimized the battery operation conditions. We set EOL_{mg} and EOL_{rq} to 100 and 500 cycles, respectively. The optimization result of controllable operation condition vector $[RMS(I_d), V_c, I_c, T] = [1.67, 4.29, 1.00, 23.22]$. That is, to use the battery over 500 cycles while maximizing the user's satisfaction in terms of effective charge capacity and charge speed, we have to maintain the battery temperature at 23.22 °C and limit the discharge stress to 1.67 A, charge voltage to 4.29 V and charge current to 1.00 A, respectively. α and β are set to 0.85 and 0.15. Determination of weighing factors should be explored further to maximize the user's satisfaction which is part of our future work.

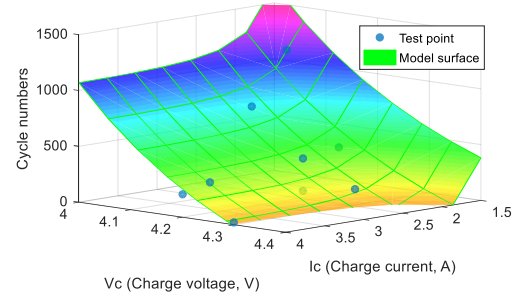


Figure 19: Predicted and measured EOL under different charge voltage and current conditions

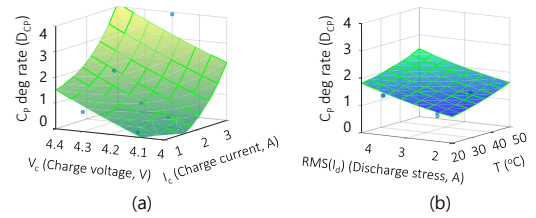


Figure 20: Computed and measured degradation rate (D_{CP}) with respect to the operating conditions

7 CONCLUSION

To diagnose and prognose batteries for their effective control, we have analyzed battery diagnostic data, predicted battery degradation, and optimized battery operating conditions. For battery prognosis, we have developed a degradation model based on the parametric OCV model and an equivalent circuit model. The thus-developed battery degradation model was used to predict battery EOL cycle and optimize battery operation conditions to guarantee the EOL warranty while maximizing battery utilization. Our evaluation with real battery data has shown the proposed schemes to yield an accurate battery degradation model.

Our method can also be applied to any type of battery cell/pack if its voltage, current, and temperature are measurable at a sufficiently high sampling rate. Positive and negative capacity parameters can be estimated based on voltage measurements and half-cell OCV, while resistance and capacitance parameters estimated if voltage, current, and temperature are available.

ACKNOWLEDGEMENT

The work reported in this paper was supported in part by the NSF under Grants CNS-1446117 and CNS-1739577.

REFERENCES

- [1] L. Lu, X. Han, J. Li, J. Hua, and M. Ouyang, "A review on the key issues for lithium-ion battery management in electric vehicles," *Journal of Power Sources*, vol. 226, pp. 272 – 288, 2013.
- [2] J. Zhang and J. Lee, "A review on prognostics and health monitoring of li-ion battery," *Journal of Power Sources*, vol. 196, no. 15, pp. 6007 – 6014, 2011.

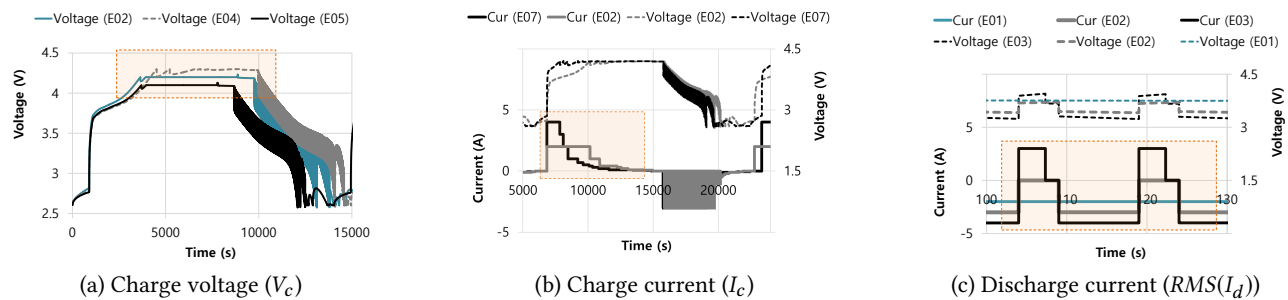


Figure 21: Test profiles with different charge/discharge currents and voltages.

- [3] X. Lin, J. Park, L. Liu, Y. Lee, A. M. Sastry, and W. Lu, "A comprehensive capacity fade model and analysis for li-ion batteries," *Journal of The Electrochemical Society*, vol. 160, no. 10, pp. A1701–A1710, 2013.
- [4] M. Chen and G. A. Rincon-Mora, "Accurate electrical battery model capable of predicting runtime and i-v performance," *IEEE Transactions on Energy Conversion*, vol. 21, no. 2, pp. 504–511, June 2006.
- [5] D. Wang, Q. Miao, and M. Pecht, "Prognostics of lithium-ion batteries based on relevance vectors and a conditional three-parameter capacity degradation model," *Journal of Power Sources*, vol. 239, no. Supplement C, pp. 253 – 264, 2013. [Online]. Available: <http://www.sciencedirect.com/science/article/pii/S0378775313005235>
- [6] L. Mai, M. Yan, and Y. Zhao, "Track batteries degrading in real-time," *Nature*, vol. 546, no. Supplement C, pp. 469 – 470, 2017.
- [7] L. He, Y. Gu, C. Liu, T. Zhu, and K. G. Shin, "SHARE: SoH-aware reconfiguration to enhance deliverable capacity of large-scale battery packs," in *ICCPS'15*, 2015.
- [8] L. He, E. Kim, K. G. Shin, G. Meng, and T. He, "Battery state-of-health estimation for mobile devices," in *The ACM/IEEE 8th International Conference on Cyber-Physical Systems*, 2017.
- [9] E. Kim, J. Lee, and K. G. Shin, "Modeling and real-time scheduling of large-scale batteries for maximizing performance," in *2015 IEEE Real-Time Systems Symposium*, Dec 2015, pp. 33–42.
- [10] B. Xu, A. Oudalov, A. Ulbig, G. Andersson, and D. Kirschen, "Modeling of lithium-ion battery degradation for cell life assessment," *IEEE Transactions on Smart Grid*, vol. PP, no. 99, pp. 1–1, 2016.
- [11] B. Saha and K. Goebel, "Modeling li-ion battery capacity depletion in a particle filtering framework," in *Conference of the Prognostics and Health Management Society*, 2009.
- [12] C. R. Birkel, E. McTurk, M. R. Roberts, P. G. Bruce, and D. A. Howey, "A parametric open circuit voltage model for lithium ion batteries," *Journal of The Electrochemical Society*, vol. 162, no. 12, pp. A2271–A2280, 2015.
- [13] M. Dubarry, C. Truchot, and B. Y. Liaw, "Synthesize battery degradation modes via a diagnostic and prognostic model," *Journal of Power Sources*, vol. 219, pp. 204 – 216, 2012. [Online]. Available: <http://www.sciencedirect.com/science/article/pii/S0378775312011330>
- [14] K. Uddin, S. Perera, W. D. Widanage, L. Somerville, and J. Marco, "Characterising lithium-ion battery degradation through the identification and tracking of electrochemical battery model parameters," *Batteries*, vol. 2, no. 2, 2016. [Online]. Available: <http://www.mdpi.com/2313-0105/2/2/13>
- [15] N. Lotfi, P. Fajri, S. Novosad, J. Savage, R. G. Landers, and M. Ferdowsi, "Development of an experimental testbed for research in lithium-ion battery management systems," *Energies*, vol. 6, no. 10, pp. 5231–5258, 2013.
- [16] E. Wood, M. Alexander, and T. H. Bradley, "Investigation of battery end-of-life conditions for plug-in hybrid electric vehicles," *Journal of Power Sources*, vol. 196, no. 11, pp. 5147 – 5154, 2011. [Online]. Available: <http://www.sciencedirect.com/science/article/pii/S037877531100379X>
- [17] M. Daigle and C. S. Kulkarni, "End-of-discharge and end-of-life prediction in lithium-ion batteries with electrochemistry-based aging models," *AIAA Infotech*, 2016. [Online]. Available: <https://doi.org/10.2514/6.2016-2132>
- [18] P. Gao, C. Zhang, and G. Wen, "Equivalent circuit model analysis on electrochemical impedance spectroscopy of lithium metal batteries," *Journal of Power Sources*, vol. 294, no. Supplement C, pp. 67 – 74, 2015. [Online]. Available: <http://www.sciencedirect.com/science/article/pii/S0378775315010666>
- [19] U. Tröltzsch, O. Kanoun, and H.-R. Tränkler, "Characterizing aging effects of lithium ion batteries by impedance spectroscopy," *Electrochimica Acta*, vol. 51, no. 8, pp. 1664 – 1672, 2006, electrochemical Impedance Spectroscopy. [Online]. Available: <http://www.sciencedirect.com/science/article/pii/S0013468605007899>
- [20] R. Ahmed, J. Gazzarri, S. Onori, S. Habibi, R. Jackey, K. Rzemien, J. Tjong, and J. LeSage, "Model-based parameter identification of healthy and aged li-ion batteries for electric vehicle applications," *SAE Int. J. Alt. Power.*, vol. 4, pp. 233–247, 04 2015. [Online]. Available: <https://doi.org/10.4271/2015-01-0252>
- [21] M. Dalal, J. Ma, and D. He, "Lithium-ion battery life prognostic health management system using particle filtering framework," *Proceedings of the Institution of Mechanical Engineers, Part O: Journal of Risk and Reliability*, vol. 225, no. 1, pp. 81–90, 2011.
- [22] J. R. Koza, *Genetic programming: on the programming of computers by means of natural selection*. MIT press, 1992, vol. 1.
- [23] D. A. Augusto and H. J. Barbosa, "Symbolic regression via genetic programming," in *Neural Networks, 2000. Proceedings. Sixth Brazilian Symposium on*. IEEE, 2000, pp. 173–178.
- [24] Tenergy. 3.7v 2200mah li-ion 18650 flat top rechargeable battery with pcb. <http://www.tenergy.com/30004>.